Migration of Natural Hydrogen from Deep-Seated Sources in the São Francisco Basin, Brazil

Frédéric-Victor Donzé, Laurent Truche, Parisa Shekari Namin, Nicolas Lefeuvre, Elena Bazarkina

geosciences

MDPI

Article

Migration of Natural Hydrogen from Deep-Seated Sources in the São Francisco Basin, Brazil

Frédéric-Victor Donzé [1,*], Laurent Truche [1], Parisa Shekari Namin [1], Nicolas Lefeuvre [1] and Elena F. Bazarkina [2,3]

1 University Grenoble Alpes, University Savoie Mont Blanc, CNRS, IRD, IFSTTAR, ISTerre, 38000 Grenoble, France; laurent.truche@univ-grenoble-alpes.fr (L.T.); parisa.shekari@gmail.com (P.S.N.); nicolas.lefeuvre@univ-grenoble-alpes.fr (N.L.)

2 Institute Néel, University Grenoble Alpes, UPR 2940 CNRS, 38000 Grenoble, France; elena.bazarkina@neel.cnrs.fr

3 Institute of Geology of Ore Deposits, Mineralogy, Petrography and Geochemistry, Russian Academy of Sciences, 119017 Moscow, Russia

* Correspondence: frederic.donze@univ-grenoble-alpes.fr

Received: 22 July 2020; Accepted: 28 August 2020; Published: 2 September 2020

Abstract: Hydrogen gas is seeping from the sedimentary basin of São Franciso, Brazil. The seepages of H_2 are accompanied by helium, whose isotopes reveal a strong crustal signature. Geophysical data indicates that this intra-cratonic basin is characterized by (i) a relatively high geothermal gradient, (ii) deep faults delineating a horst and graben structure and affecting the entire sedimentary sequence, (iii) archean to paleoproterozoïc basements enriched in radiogenic elements and displaying mafic and ultramafic units, and (iv) a possible karstic reservoir located 400 m below the surface. The high geothermal gradient could be due to a thin lithosphere enriched in radiogenic elements, which can also contribute to a massive radiolysis process of water at depth, releasing a significant amount of H_2. Alternatively, ultramafic rocks that may have generated H_2 during their serpentinization are also documented in the basement. The seismic profiles show that the faults seen at the surface are deeply rooted in the basement, and can drain deep fluids to shallow depths in a short time scale. The carbonate reservoirs within the Bambuí group which forms the main part of the sedimentary layers, are crossed by the fault system and represent good candidates for temporary H_2 accumulation zones. The formation by chemical dissolution of sinkholes located at 400 m depth might explain the presence of sub-circular depressions seen at the surface. These sinkholes might control the migration of gas from temporary storage reservoirs in the upper layer of the Bambuí formation to the surface. The fluxes of H_2 escaping out of these structures, which have been recently documented, are discussed in light of the newly developed H_2 production model in the Precambrian continental crust.

Keywords: native hydrogen; H_2 exploration; gas seeps; H_2 venting; radiolysis; serpentinization; draining faults; intra-cratonic basin

1. Introduction

The natural production of molecular hydrogen (hereafter hydrogen or H_2) has drawn increasing scientific attention due to the central role this molecule plays in fueling the deep subsurface biosphere or promoting the abiotic synthesis of organic molecules (Truche et al., 2020 [1]). Natural H_2 sources may also represent a new attractive primary carbon free energy resource (Smith, 2002 [2]; Smith et al., 2005 [3]; Truche and Bazarkina, 2019 [4]; Gaucher, 2020 [5]). This latter industrial perspective has motivated recent H_2 exploration studies in ophiolite, peralkaline, Precambrian shields and intra-cratonic geological settings (see review by Zgonnik, 2020 [6]).

Natural hydrogen (also known as native hydrogen) sources have been identified for several decades in seafloor hydrothermal vents, and hyperalkaline springs in ophiolite massifs. Serpentinization of ultramafic rocks is the water–rock interaction process responsible for H_2 generation in these contexts (Neal and Stranger, 1983 [7]; Coveney et al., 1987 [8]; Abrajano et al., 1990 [9]; Charlou et al., 1996 [10]; Seewald et al., 2003 [11]). However, the recent discoveries of intra-cratonic H_2 seepages and accumulations with no obvious link to an ultramafic formation challenge our current understanding of H_2 production and fate in the crust (Larin et al., 2015 [12]; Zgonnik et al., 2015 [13], Prinzhofer et al., 2018 [14]). To date, there is no in-depth understanding of the hydrogen system from source to seep in these latter geological settings. When not fortuitous, as in the Taoudeni Basin in Mali (Prinzhofer et al., 2018 [14]), the discoveries of new H_2 seepages were made thanks to the satellite detection of sub-circular soil depressions displaying vegetation anomalies, e.g., Borisoglebsk in Russia (Larin et al., 2015 [12]) and Carolina Bay in the US (Zgonnik et al., 2015 [13]). These surface features are the only evidence used to detect these H_2 seepages. This limited understanding of the H_2 systems, and this lack of robust pathfinders prevents the development of a methodic exploration strategy or resource assessment in these environments.

The São Francisco Basin belongs to this short list of intra-cratonic basins where H_2 seepages have been discovered. There, hydrogen gas vents from slight topographic depressions that are circular and barren of vegetation and, in one of them, the recorded H_2 concentrations range from 50% to 80% (Prinzhofer et al., 2019 [15]; Cathles and Prinzhofer, 2020 [16]). In the area of the São Francisco Basin, Flude et al., (2019 [17]) also, recorded up to 20% H_2, mostly accompanied with N_2 and several percent of CH_4, in the gas mixture from the head of exploration wells and natural gas seeps.

The São Francisco basin provides one of the first H_2 case studies where geological information can be collected with a sufficient level of detail to provide the primary elemental bricks that may compose the H_2 system in intra-cratonic basins. Here, we review the different layers of information that compose a supposed H_2 system in this basin and lay the foundation of a H_2 exploration guide.

2. The São Francisco Basin

Located in the Brazilian states of Minas Gerais and Bahia, the São Francisco Craton presents rocks dating back to the Paleoarchean, to the Cenozoic, and several Precambrian sedimentary successions (Heilbron, 2017 [18]) (Figure 1). The basement is mostly composed of Archean TTG (Tonalite–Trondhjemite–Granodiorite) rocks, granitoids and greenstones belts (Anhaeusser, 2014 [19]) together with Paleoproterozoic plutons and supra-crustal successions. This polycyclic substratum, assembled during late Neoarchean times under high-grade metamorphic conditions, is intruded by late tectonic K-rich granites, mafic-ultramafic units, and mafic dikes (Teixeira et al., 2017 [20]). The Southern part of the São Francisco Craton consists of several gneiss complexes and greenstone belts from the Mineiro orogeny.

The sedimentary cover is made up of units younger than 1.8 Ga: the São Francisco basin (Southern part), the Paramirin Aulacogen (Northern part) and the Recôncavo–Tucano–Jatoba rift (Northeastern part) (Heilbron et al., 2017 [18]). Besides these Proterozoic sedimentary successions, the São Francisco basin also contains Phanerozoic units (Permo-Carboniferous and Cretaceous rocks).

Along the southern edge of the São Franciso basin, the Bambuí Group fills a series of buried grabens. The Bambuí strata exposed along the area of interest in this study are generally flat lying and cover more than 300,000 km^2. The entire basin is covered by 450 to 1800 m-thick Neoproterozoic to Cambrian sedimentary successions, which are unconformably overlying the Archean-Paleoproterozoic basement (Delpomdor et al., 2020 [21]) (Figure 1b).

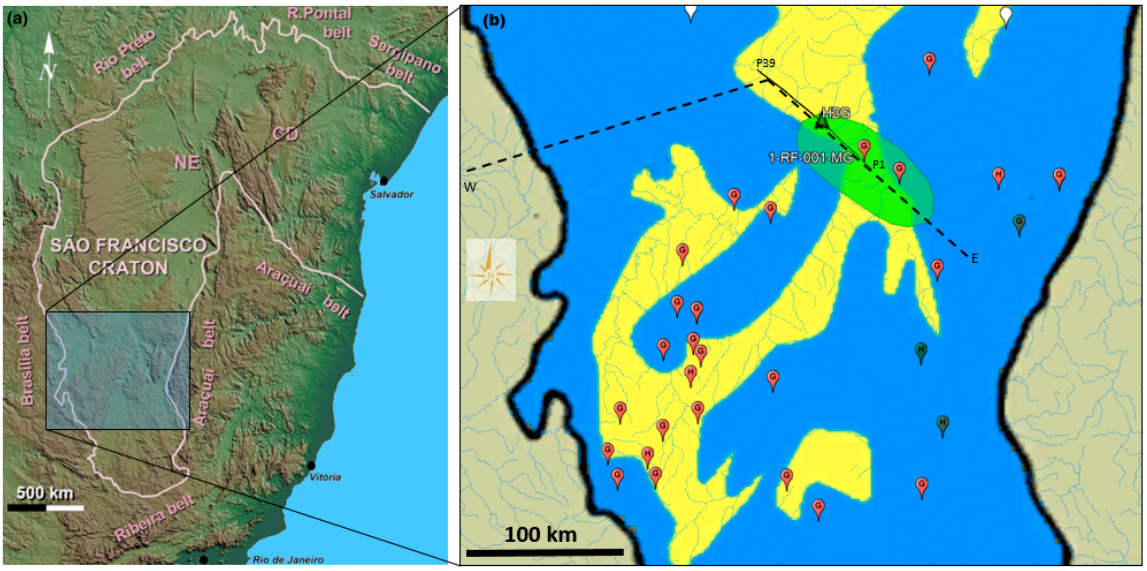

Figure 1. (**a**) Digital elevation model of southeastern Brazil, showing the topography associated with the São Francisco Craton outlined by the pink line (From Heilbron et al., 2017 [18]). (**b**) Simplified geological map (Serviço Geológico do Brasil) of the Southern part of the São Francisco Basin, outlined by the black line, with the Bambuí group in Yellow, the Phanerozoic cover in blue. Gas seepages (H_2, N_2, He, Hydrocarbons) have been observed during field investigations inside the green ellipse (Curto et al., 2012 [22]) and the triangle H2G corresponds to the gas seepage presented in Figure 2 (Prinzhofer et al.; 2019 [15]). The red markers, including the 1-RD-001-MG well, indicate locations of the exploration wells. The E–W (East–West) black dash line corresponds to the seismic sections presented in Figure 3. The solid black line linking the P1 and P39 white markers corresponds to the Magnetotelluric stations for the MT1 line set up in São Francisco Basin by Solon et al. (2015 [23]).

3. H_2 Seepages in the Bambuí Group in the Southern Part of the São Francisco Basin

To constrain the magnitude of the H_2 emission, a permanent monitoring station has been installed in a depression located 16 km North-North East of Santa Fé de Minas in the State of Mina Gerais (Prinzhofer et al., 2019 [15]) (Figure 2). The recorded emission rates range from 7000 m^3 to 178,000 m^3 of H_2 per day with H_2 concentrations in the venting gas in the order of 1000 ppm (Cathles and Prinzhofer, 2020 [16]).

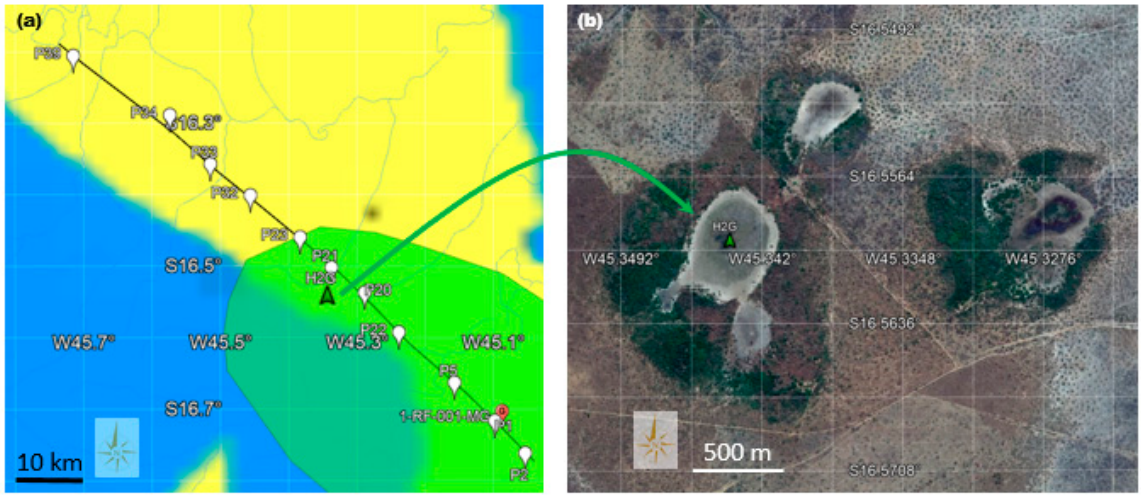

Figure 2. (**a**) Magnetotelluric stations for the MT1 line set up in São Francisco Basin by Solon et al. (2015 [23]) with the location of well 1-RF-001-MG, from Figure 1b. (**b**) H_2 seepages (H2G) observed in circular depression zones (16°33.605′ S; 45°20.620′ W) (Prinzhofer et al., 2019 [15]).

In the same area, various geophysical data acquisitions have been previously obtained from surface monitoring or exploration wells. Seismic and magnetotelluric sections show the distribution of the main stratigraphic units across the São Francisco basin (e.g., Romeiro-Silva and Zalán, 2005 [24]; Reis and Alkmim, 2015 [25]; Solon et al., 2015 [23]) (Figure 1b).

The Bambuí group includes seven stratigraphic units. Logs from the 1-RF-001-MG well, located near station P1 on line MT1 (Figure 2a), provide quantitative information regarding the thickness of each geological layer to a depth of 1848 m with the sequences listed in Table 1. The depositional age of the Bambuí Group, especially its lower part, remains controversial, e.g., the estimated date varies from 560 Ma to 762 Ma for the lowermost part of the Sete Lagoas (Delpomdor et al., 2020 [21]).

Table 1. Simplified interpretation of the well log data from the Petrobras' well 1-RF-1-MG (From Solon et al., 2015 [23]).

Depth	Composition	Lithology
surface to ~30 m ~30 m to ~320 m	• Siltstones and sandstone. • Mainly composed of sandstone, siltstone, mudstone and shale.	Serra de Saudade Formation
~320 m to ~480 m ~480 m to ~680 m	• Limestone. • Intercalations of limestone and shale.	Lagoa do Jacaré Formation
~680 m to ~980 m ~980 m to ~1200 m	• Mainly composed of siltstone. • Mainly consisting of limestone and dolomite.	Serra de Santa Helena Formation
~1200 m to ~1240 m	• Mainly consisting of limestone and dolomite.	Sete Lagoas Formation
~1240 m to ~1640 m below ~1640 m	• Composed of intercalations of shales and limestone, conglomerates and diamictite. • Composed of shale, limestone and conglomerate.	Jequitaí Formation

4. A Possible Deep Origin for H_2

In addition to H_2 venting at location H2G (Figure 2b), He concentrations (5 ppm above atmospheric reference value) measured by Prinzhofer et al. (2019 [15]) at a depth of 1 m, suggest a possible gas migration from deep horizons, where He is generated. Other analyses of gas sampled at the surface, from the head of the exploration wells drilled in the São Francisco basin confirmed that, besides high concentrations of H_2 (up to ~20%), He (>1%) is also present, in association with methane-dominated hydrocarbons and N_2 (Flude et al., 2019 [17]). Stable isotope data also suggest an abiotic origin for the methane, while He isotopes reveal a strong crustal signature ($^3He/^4He < 0.02$ R/Ra) (Flude et al., 2019 [17]). The nucleogenic ^3He from the decay of ^6Li could account for the $^3He/^4He$ ratios found in the head of the exploration wells drilled in the São Francisco basin, i.e., close to R/Ra = 0.01 for an average granitic crust. Moreover, Neon isotope data also suggest the presence of an Archaean crustal component in the gases, indicating that a component of the gas has likely originated from the underlying crystalline basement, or within Archaean-derived sedimentary rocks (Flude et al., 2019 [17]).

The natural production of the continental H_2 can be of various origins (Guélard et al., 2017 [26]). Studies in deep mines from the Witwatersrand basin (South Africa) and the Timmins basin (Ontario, Canada) have suggested a link between dissolved H_2 and the radiolytic dissociation of water (Lin et al., 2005a [27]). In addition to radiolysis, hydration of ultramafic rocks coupled to H_2O reduction could also be responsible for H_2 generation in Precambrian shields (Goebel et al., 1984 [28]; Sherwood Lollar et al., 2014 [29]). For example, the serpentinization of the gabbroic basement has been proposed as the process responsible for H_2 production in Kansas (Coveney et al., 1987 [8]).

Radiolysis and serpentinization both require specific environments, which can be identified from geophysical and mineralogical investigations. Regarding the São Francisco basin, we detail these two possible processes of H_2 formation in the following subsections.

4.1. Production of H_2 by Water Radiolysis

Distinct Archean gneissic–granitic complexes characterize the Southern part of the São Francisco Craton basement. They constitute a medium- to high-grade metamorphic terrain that crops out from the Quadrilátero Ferrífero towards the west, and mainly comprises TTG rocks, migmatites and K-rich granitic plutons (Teixeira et al., 2017 [20]). These rocks record deformational and metamorphic Archean episodes (from 2.55 Ga to over 3.3 Ga). It is known that the crystalline basement, rich in radiogenic elements and particularly this type of old basement Precambrian rock, represents potentially fertile deep-seated sources of H_2 (Parnell et al., 2017 [30]; Sherwood Lollar et al., 2014 [29]). Indeed, molecular hydrogen production from water radiolysis requires the presence of radiogenic elements such as U, Th or K, which split the water molecules by ionizing radiation to produce molecules of H_2. For the São Francisco Craton, the measured concentrations of uranium (U), thorium (Th) and potassium (K) are presented in Table 2. The Bambuí Group exhibits intermediate-to-high K and Th contents, while U-levels are around 2.5 ppm (Reis et al., 2012 [31]).

Table 2. Measured concentrations of Uranium, Thorium and Potassium.

Radioelement	Archean Granulitic Rocks of the Jequie Complex [1]	Brauna Kimberlite Present in the Archean Basement [2]	Bambuí Group
Uranium (U)	up to 5 ppm	up to 4.81 ppm	up to 2.5 ppm
Thorium (Th)	up to 100 ppm	up to 35.8 ppm	up to 16 ppm
Potassium (K)	up to 4.5%	NA	up to 3%

[1] Sighinolfi et al., 1982 [32]; [2] Donatti-Filho et al., 2013 [33].

In a coarse-grained rock like granite, beta-irradiation from K is more prone to affect inter-granular fluid than the shorter-range alpha irradiation from U. Since K is also more pervasively distributed than U in granite, it can contribute to a larger scale radiolysis process.

Given the rather consistent range of U, Th, and K concentrations reported in the São Francisco Basin, we could expect in this zone a production rate of radiolytic H_2 in water ranging from 10^{-8} to 10^{-7} nmol·L^{-1}·s^{-1} (Lin et al., 2005b [34]). The methodology proposed by Sherwood Lollar et al. (2014 [29]) to estimate the contribution of the Precambrian continental crust to H_2 production via radiolysis may then be applied to infer the regional H_2 flux. The total radiolytic H_2 production rate in water-filled fractures of the Precambrian crust was estimated to range from 0.16 to 0.47 × 10^{11} mol·yr^{-1} for a corresponding surface area of 1.06 × 10^8 km^2. Given the surface area of the Sao Francisco Basin of 300,000 km^2, this corresponds to a H_2 diffusive flux of 0.45 to 1.34 × 10^8 mol·yr^{-1}, i.e., 90 to 266 tons·yr^{-1}.

4.2. Production of H_2 by Serpentinization or Hydration

Serpentinization occurs when meteoric or oceanic waters alter ultramafic rocks originating from the Earth's mantle, such as peridotites and volcanic rocks. These rocks undergo changes in pressure and temperature conditions, which cause them to react in the presence of water (Schlindwein and Schmid, 2016 [35]; Horning et al., 2018 [36]): They are oxidized and hydrolyzed with water into serpentine, brucite and magnetite. The anaerobic oxidation of Fe(II) by the protons of water leads to the formation of H_2 (Foustoukos et al., 2008 [37]; Proskurowski et al., 2008 [38]). In Precambrian rocks, Sherwood Lollar et al. (2014 [29]) propose that for the totality of the Precambrian crust (i.e., 1.06 × 10^8 km^2) around 0.2 to 1.8 × 10^{11} mol·yr^{-1} of H_2 are produced by hydration. Here again, rescaling these values for the São Francisco basin (300,000 km^2), we obtain a H_2 production rate from hydration reactions of 0.56 to 5.09 × 10^8 mol·yr^{-1}, i.e., 113 to 1018 tons·yr^{-1}.

Favorable conditions to produce H_2 by a serpentinization process would imply the presence of low-silica mafic and ultramafic rocks as well as an optimum temperature.

4.3. Presence of Ultramafic Rocks

From the seismic section that crosses the São Francisco Craton from East to West (Figure 1b), the interpretations done by several authors agree on the identification of the Bambuí group (Figure 3). This unit is about 1200–1300 m deep in the area of the H2G seepage zone and lies on the Jequitaí formation which itself lies on the poorly identified older Proterozoic succession, the Macaúbas and possibly the Espinhaço formations (Solon et al., 2015 [23]).

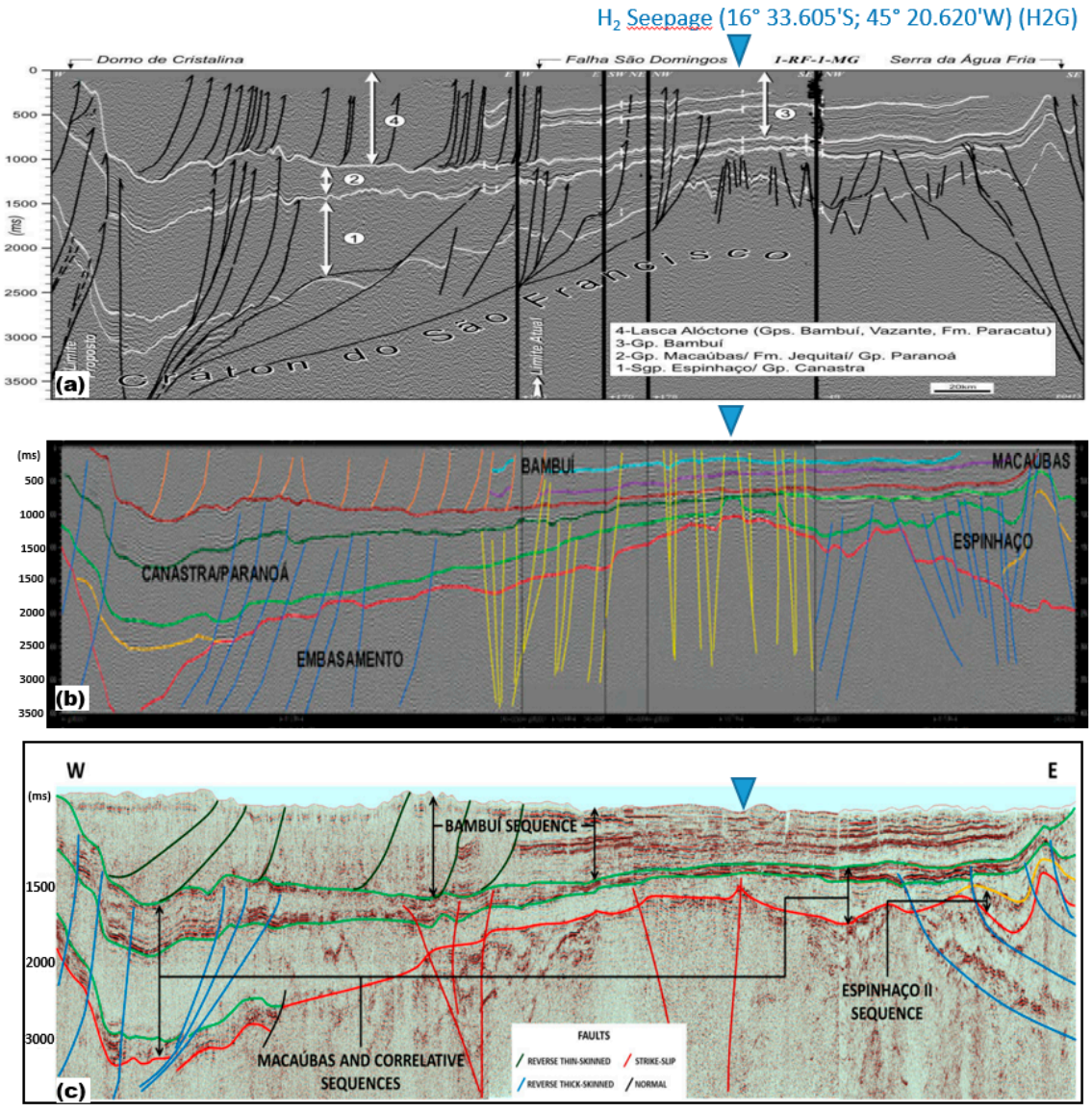

Figure 3. Three interpretations of the same reflection seismic section across the São Francisco craton (see Figure 1b for the location) from East "E" to West "W". From top to bottom: (**a**) Romeiro-Silva and Zalán (2005 [24]), (**b**) Coelho et al. (2008 [39]) and (**c**) Alkmim and Martins-Neto (2012 [40]). The locations of the exploration well A-RF-1-MG are shown in (**a**) and the gas seepage H2G (blue triangle) is reported for all cases. On all illustrations, the depth is expressed in two-way travel time (TWT).

The basal Paranoá–Upper Espinhaço sequence consists of continental sediments and volcanic rocks associated with anorogenic plutons. Mesoproterozoic anorogenic magmatism associated with multiple rifting episodes might represent a manifestation of the Columbia supercontinent breakup, which started around 1.6 Ga and ended between 1.3 and 1.2 Ga (Reis et al., 2017a, b [41,42]). The Espinhaço Supergroup is exposed on the East of the São Francisco Basin. The two basal formations of the Espinhaço sequence

are composed of alluvial sandstones, conglomerates and pelites and form a ca. 300-m-thick of two coarsening-upward sequences. Despite the potential presence of K-rich alkaline volcanic and intrusives rocks (Chemal et al., 2012 [43]), this formation does not seem suitable for H_2 production.

The basement rocks of the São Francisco basin are dominated by Archaean to Palaeoproterozoic migmatites, amphibolite to granulite-grade gneisses, and granite–greenstones (Teixeira et al., 2017 [20]). For example, the Rio Itapicuru low-grade supra-crustal greenstone belt has several lithostratigraphic subdivisions, including a basal mafic volcanic unit composed of massive and pillowed basaltic flows intercalated with chert, banded iron-formation, and carbonaceous shale (Oliveira et al., 2019 [44]). The banded iron-formation is mainly composed of oxidized iron Fe(III) forming a possible mix of hematite and magnetite, which can produce a strong magnetic anomaly (Pereira and Fuck, 2005 [45]) (purple zones in Figure 4).

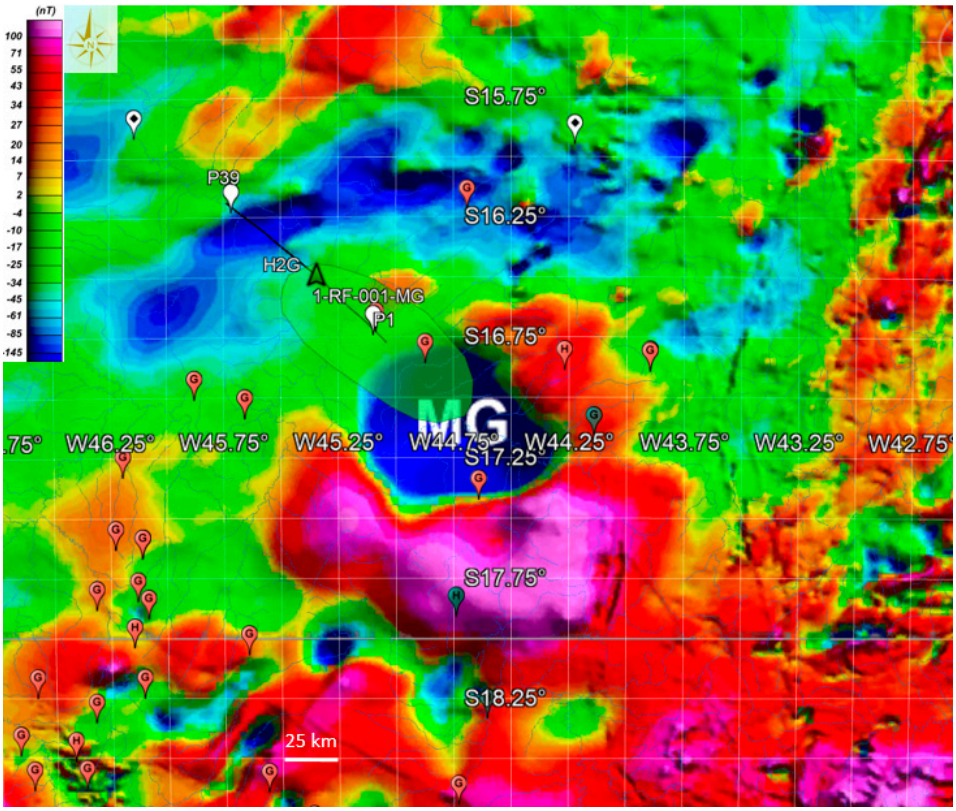

Figure 4. Magnetometric map (modified from Correa, 2019 [46]). Note that "MG" stands for "Minas Gerais".

In this area, the Bouguer anomaly map exhibits predominantly negative anomalies (Figure 5) which correlate with granitoids resulting from the crustal rejuvenation of the area, associated with partial re-fusion of the crust during past thermal events. This also suggests that major magmatic sequences affected the basement of the southern part of the São Franscico Basin, which is compatible with the magnetic anomalies (Figure 4). Since the Quadrilátero Ferrífero (a mineral-rich region with extensive deposits of iron ore) and the "greenstone" belts present the same gravimetric signature, they could have the same origin (Pinto et al., 2007 [47]). Here again, the basement rock composition presents a high potential for H_2 production.

4.4. Temperature Ranges at Depth

The potential presence of ultramafic rocks within the area of gas seepages, could suggest a serpentinization process, but to be active, this process would require a favorable range of temperatures. Crustal thermal models have been developed to examine the implications of the observed intra-cratonic

variations in heat flow across the São Francisco Basin (Alexandrino et al., 2008 [48]). The thermal models take into consideration the variation of thermal conductivity with temperature. It is thus possible to get the temperature distribution calculated along a large profile that crosses the São Francisco Basin. It turns out that our zone of interest in the São Francisco Basin, exhibits an abnormally high heat flow value for a craton (Figure 6). In the gas seepage zone (green ellipse in Figure 5), the temperature gradient is about 25 °C/km (Alexandrino et al., 2008 [48]). The optimum temperature for serpentinization was found to be around 250–300 °C with a maximum production of magnetite (Klein et al., 2013 [49]). However, some experimental data suggest that below 150 °C, H_2 can still be produced through the formation of Fe^{3+} oxi-hydroxides (Mayhew et al., 2013 [50]; Miller et al., 2017 [51]), with the formation of H_2 being possibly catalyzed by the surface of spinel-structure minerals occurring in ultramafic rocks. In such thermal conditions, H_2 could still be produced at a low rate, at a depth lower than 6 km, near the gas seepage zone, and the optimum depth for its production would be at 10–12 km.

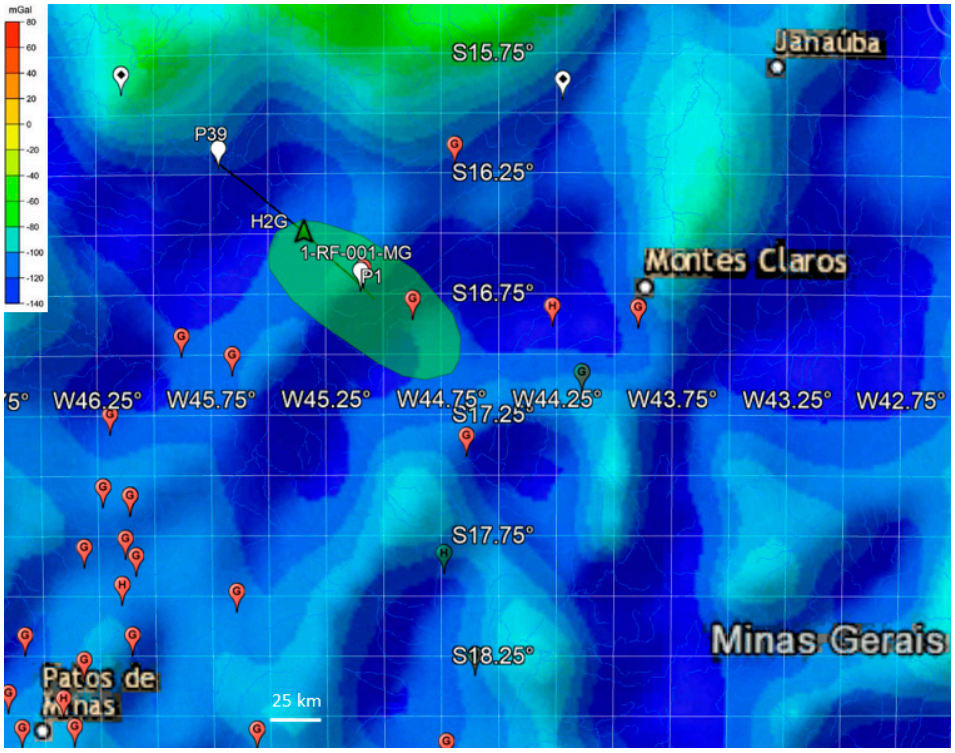

Figure 5. Bouguer anomaly map in the São Francisco Basin within the studied zone (modified from Oliveira and Andrade, 2014 [44]).

4.5. Possible H_2 Bubbling at Depth

Once produced by fluid–rock interaction processes (oxidation) at depth, H_2 can migrate as a dissolved component. The solubility of H_2 in aqueous solutions is rather low and drops when T and P decrease when approaching the surface (Figure 7d). The possible mechanism of H_2 discharge, concentrating, and transport upward to the lower T–P where H_2 is less reactive is solution boiling, i.e., formation of the vapor phase coexisting with the liquid phase. The concentrations of H_2 in vapors are many orders of magnitude higher than that in the liquid (Bazarkina et al., 2020). At the same time, rock permeability is much higher for gas-rich vapors than for salt-rich liquids. Bubble formation is a function of T, P, total salinity, and gas saturation. Thus, during fluid ascent upward to the lower T–P, gas bubble formation is favored (Figure 7d). Periodicity of H_2 emission at the surface reported by Prinzhofer et al. (2019) could be related to the kinetics of fluid–rock interaction at depth, further time-dependent bubble accumulation, and the final periodical ejections similar to those described in geysers.

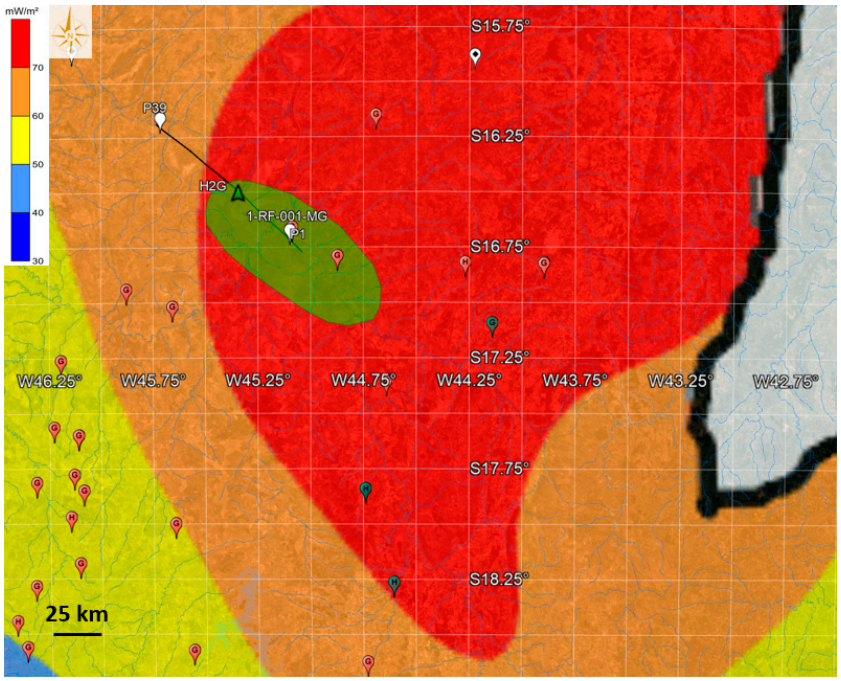

Figure 6. Heat flow map in the São Francisco Basin within the studied zone (modified from Alexandrino and Hamza, 2012 [52]).

5. Draining Fault System in the São Francisco Basin

Deep faults serve as significant channels for deep fluids to ascend into and through the crust and the $^3He/^4He$ ratio can be used to estimate the flow rate of mantle fluids through the fault zones (Kennedy et al., 1997 [53]). Since the $^3He/^4He$ signature seems to be of crustal origin in the São Francisco basin (Flude et al., 2019 [17]), the migration path followed by the H_2 mostly crosses the sedimentary cover without major changes of the ratio value. This weak interaction with the Bambuí sequences could be due to a high flow rate value along the faults. This could be possible if the faults form direct drains from the basement to the surface assuming a sufficiently high value of permeability.

Several interpretations of the available seismic data have been proposed for the fault systems (Figure 3) (e.g., Romeiro-Silva and Zalán, 2005 [24]; Coelho et al., 2008 [39] and Alkmim and Martins-Neto, 2012 [40]). Nevertheless, the São Francisco basin seems to encompass different tectonic elements such as the Proterozoic rift structures, Neoproterozoic foreland f–t-belts and Cretaceous rift structures (Reis and Alkmim, 2015 [25]). The rift structure that cuts across the central portion of the basin is characterized by a system of major NW–SE faults. One could expect that the deep-rooted faults in the graben structures (Precambrian sequence), which have been reactivated during the Neoproterozoic Macaúbas basin-cycle, could cross most of the sedimentary formation. As a major fault system, they may control the drainage at all depths and delineate some morphological features observed on satellite imagery and digital elevation models (Reis et al., 2017b [42]).

If these faults cross different geological layers, mainly shales, sandstones and limestones, their permeability values can range from 10^{-19} to 10^{-13} m^2 (Donzé et al., 2020 [54]). In terms of hydraulic conductivity for the water carrying the gas and neglecting the contribution of temperature, this could correspond to a value as high as 10^{-6} m/s. This means that in the fastest scenario, the fluid could take less than 100 years to migrate across the Bambuí sedimentary layer through a fault system.

6. Possible Temporary Shallow Zones of H_2 Accumulation

The pressure variation observed at 1 m depth in the São Francisco basin (Prinzhofer et al., 2019 [15]), with a momentary increase in H_2 pressure, could indicate that the H_2 systems are active.

There is only a small temperature window where H_2 may remain stable over a long time. This window corresponds to a T range where abiotic redox reactions such as thermochemical sulfate reduction or carbonate reduction (e.g., Fisher Tropsh type reaction) are slow (Truche et al., 2009 [55]), and where bacteria are inactive. Such a T range can be roughly approximated to be 100–200 °C. Since these temperature conditions are not met at shallow depth, H_2 will probably not survive to long residence time. Despite this fact, previous studies of H_2 seepages often indicate that the hydrogen systems are active, and transient accumulations of hydrogen at relatively shallow depth can be observed (Prinzhofer et al., 2018 [14], Goebel et al., 1984 [28]; Guélard et al., 2017 [26]). These observations may suggest a constant recharge of the aquifers by H_2 flowing from deeper levels of the basin.

The circular depression where H_2 seepage is observed (Figure 2b) could be related to a sinkhole structure resulting from a chemical dissolution process at depth. If so, these depressions will contain standing water connected with a ground-water reservoir contained in karst (De Carvalho et al., 2014 [56]). The presence of resistive carbonate and calcareous rocks was inferred from ~320 m to ~480 m followed by a layer of intercalated shales and sandstones (Solon et al., 2015 [23]). This carbonate layer, which corresponds to the Lagoa do Jacaré carbonate layer, exhibits a potential karst system according to the outcrops located East of the São Francisco Basin (Dos Santos et al., 2018 [57]).

Assuming a karst system at depth, this could imply a high level of porosity favorable for a massive storage volume of an aquifer. Since karst features are controlled by structural heterogeneities, such as faults and fractures, which influence fluid flow, they can provide preferential pathways for geofluids with the development of secondary porosity. This could agree with the fact that the circular depressions where H_2 is venting are aligned along a major fault (Cathles and Prinzhofer, 2020 [16]).

7. Putting It All Together: A Potential H_2 System within the São Francisco Basin

The first key point is related to potential source areas, e.g., the presence of both ultramafic and U, Th and K-rich rocks. The presence of Archean greenstone belts containing ultramafic rocks, TTG, migmatites and K-rich granitic plutons represent excellent H_2-producing zones either via serpentinization, or water radiolysis. Magnetic (Figure 4) and Bouguer (Figure 5) anomalies are compatible with the presence of ultramafic rock producing H_2. Temperature conditions also seem favorable for the serpentinization process: with a temperature gradient of 25 °C/km (Alexandrino et al., 2008 [48]), the optimum range of temperature would be expected at a depth of 10 km, with possible lower rate processes at a shallower depth.

The second key point is the structural/tectonic context and the presence of faults deeply rooted in the basements capable of draining a potential deep and scattered source. All interpretations of the seismic profile of the zone of interest suggest the presence of deep faults following the graben structures (Figure 3): they can be able to drain hydrogen produced at depth where the Pressure–Temperature conditions are optimal. Some interpretations suggest that some of these faults could cross the entire sedimentary sequence (Coelho et al., 2008 [39]), producing gas seepages directly at the surface. Some others predict that these faults could reach some potential shallow carbonated reservoirs (Romeiro-Silva and Zalán, 2005 [24]). These deep faults could also only reach the unconformity zone which composes the boundary between the sedimentary basin and basement (Alkmim and Martins-Neto, 2012 [40]).

The third key point concerns the storage areas (i.e., reservoirs) of H_2 at depth. As mentioned previously, the interface between the basement rocks and the sedimentary layers could represent a potential zone of accumulation. The interface is composed of the Macaúbas and the Espinhaço formations. The Macaúbas sequence is made up of sandstones, pelites, diamictites, carbonates, basic volcanic rocks, and metamorphosed banded iron formations (Alkmim et al., 2012 [40]), whereas the Espinhaço formation is a quartz–arenite dominated package. The presence of the Paranoá–Upper Espinhaço quartzite, which is tectonically uplifted, can facilitate the occurrence of sandstone reservoirs with appreciable permeability and porosity. Thus, potential reservoir rocks could be found among siliciclastics of the Macaúbas–Paranoá Megasequence (Solon et al., 2015 [23]).

An interesting characteristic of the deep topography is that the seepage zone H2G is located near the apex of the basement rock in the central part of the basin (see Figure 3). As the H_2 charged fluid reaches the Macaúbas/Espinhaço formations, it migrates along the unconformity toward this highest point before escaping to the surface in the green seepage zone (Figure 2). On its way to the surface, H_2 can also be temporarily trapped in the Sete Lagoas formation and at a shallower depth, inside the Lagoa do Jacaré formation. The permeability value of the Sete Lagoas Larst aquifer formation is estimated to range between 10^{-14} m^2 and 10^{-9} m^2 (Galvão et al., 2015 [58]). As for the Lagoa do Jacaré formation, very low permeability and porosity values were found in the Petrobras well 1-RF-1-MG. The presence of faults, possibly connecting all these reservoirs with the surface could explain the apparent structural control of the distribution of the known gas seepages (Curto et al., 2012 [22]). Nevertheless, the presence of sinkholes in the H2G seepage area suggests the existence of a shallow local karst formation, which could constitute a temporary reservoir for H_2.

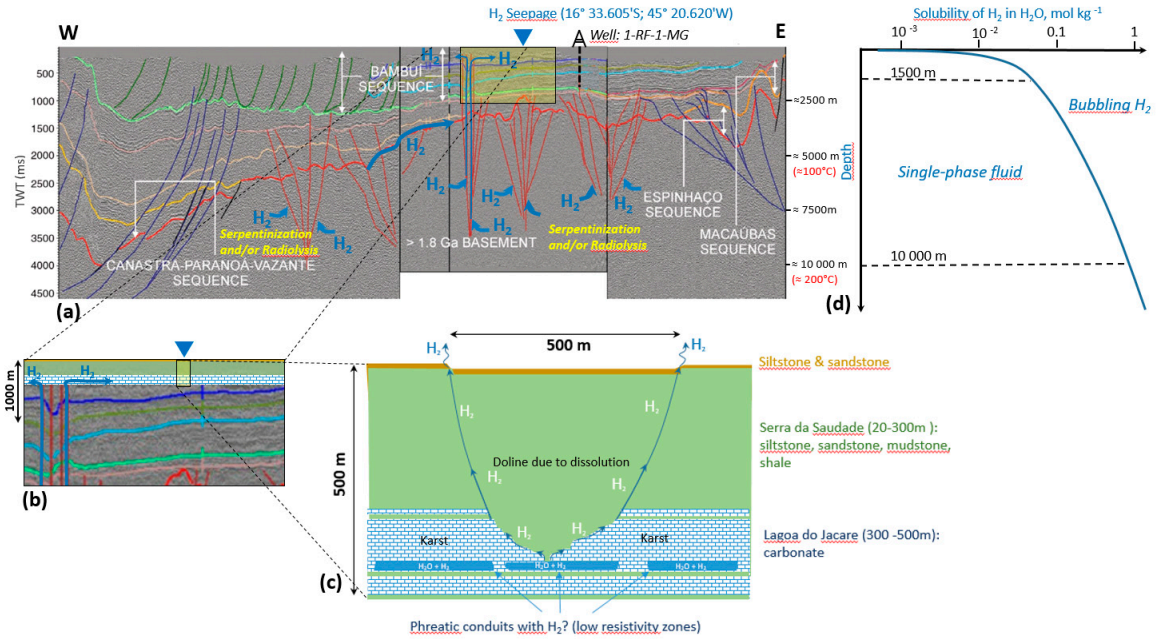

Figure 7. Conecputal model of the H_2 cycle in the Sao Francisco Basin. (**a**) Interpretated seismic section (Martins-Neto, 2009). (**b**) Zoom of the upper part of the Bambui sequence. (**c**) Possible presence of a karst structure according to the presence of sinkholes (Figure 2). (**d**) Calculated solubility of H_2 in H_2O vs. depth (Bazarkina et al., 2020 [59]).

Thus, surface seepages may be either in connection with the source rock or with intermediate leaking reservoirs since these two configurations are present in this area. A summary of H_2 migration from sources to seeps in the São Francisco basin is presented in Figure 7.

8. Discussing the H_2 Production from Radiolysis and Hydration Reactions in the São Francisco Basin

Combining the H_2 production rate from water radiolysis and hydration reactions assessed in the previous sections, we obtain an estimate of 1.01 to 6.43 × 10^8 mol·yr^{-1} H_2 production, i.e., ~200 to 1300 tons·yr^{-1} (Table 3). Cathles and Prinzhofer (2020 [23]) considered the local flux rate in the H2G seepage zone (Figure 2b) to range from 7000 to 178,000 m^3 per day. At a temperature of 21 °C and a pressure of 1 atm, these values correspond to 0.105 to 3.68 × 10^9 mol·yr^{-1}, i.e., 213 to 5400 tons·yr^{-1} (Table 3). Since the expulsion rate of H_2 is almost certainly not steady, the episodic rate measured in the H2G vent might be overestimated.

Table 3. Estimated H_2 flow rate production (tons·yr^{-1}).

System	$\times 10^9$ mol·yr^{-1}	tons·yr^{-1}	Reference
São Francisco basin (radiolysis and hydration combined)	0.101–0.643	204–1284	This study
H2G seepage zone São Francisco basin	0.105–3.68	213–5400	From Cathles and Prinzhofer, 2020 [16]
Rainbow hydrothermal field	~0.1	200	Charlou et al., 2010 [60]
Ultramafic vents along the Mid-Oceanic ridges	~10–100	20,000–200,000	Keir, 2010 [61]; Cannat et al., 2010 [62]
Global Precambrian continental lithosphere: (radiolysis and hydration combined)	36–227	72,000–454,000	Sherwood Lollar et al., 2014 [29]

In comparison, on the Mid-Atlantic Ridge (MAR), the total H_2 discharge at the Rainbow hydrothermal field is estimated to be ~10^8 moles H_2 per year, i.e., ~200 tons·yr^{-1} (Charlou et al., 2010 [60]) (Table 3). At a larger scale, the H_2 flux from all high-temperature basaltic vents along the MAR has been estimated at ~10^9–10^{10} mol·yr^{-1}, whereas the H_2 flux from high-temperature ultramafic vents along the Mid-Oceanic Ridge (MOR) has been estimated at ~10^{10}–10^{11} mol·yr^{-1} (Table 3) (Keir, 2010 [61]; Cannat et al., 2010 [62]), i.e., 20,000 to 200,000 ton.yr^{-1}.

According to our calculations, which are based on the model developed by Sherwood Lollar et al. (2014 [29]) for the Precambrian continental lithosphere, the maximum H_2 production rate from the basement rocks of the São Francisco Basin is within the same order of magnitude as the H_2 flux of one sinkhole of 500 m in diameter (H2G zone). This latter H_2 venting site would also represent from 0.047% to 7.5% of the global estimated H_2 production from the Precambrian continental Lithosphere. This large discrepancy in the results leads us to conclude that there is a need to increase the accuracy of hydrogen flux estimates through long term monitoring of soil gas migration according to different methodologies and/or to revisit the global models.

9. Conclusions

Hydrogen exploration requires a combination of the techniques and data used for both conventional petroleum and mining exploration. The first elementary bricks we provide here to evaluate the sources, migration and trapping are certainly not enough, but the following general guidelines will be extremely valuable in targeting the fertile H_2 area in intra-cratonic areas.

Explore in old provinces where basement rocks are Archean to Paleoproterozoic. Use lithologies (ultramafic rocks, U-, Th-, K-rich rocks), and He (R/Ra) as pathfinders for the H_2 generation potential. Carefully consider the local geothermal gradient as it may be of use to infer fertile zones for active serpentinization.

Identify the location of faults deeply rooted in the basement, such as horst and graben structures. Pay attention to the topography of the unconformity, which represents both a major drainage and trapping area.

Target relatively shallow traps. As for He, H_2 partitions into gas are better at a shallow depth. Surface rounded depressions, karsts and sinkholes seem to represent favorable collecting zones prior to H_2 escaping into the atmosphere. A field investigation based on electromagnetic and gravimetric prospections could help to characterize the structure of the sinkhole at depth in order to set up a geotechnical drilling at the right location. Such boreholes, carried out in the first hundreds of meters, could provide valuable information on the H_2 concentration gradient down to the upper karstic formation, which is often not possible from classical oil and gas exploration well drilling.

Dedicated exploration of boreholes is definitely required to improve this preliminary exploration guide and to strengthen the accuracy for H_2 flux measurements. Additional constraints on the

H_2–accompanying gases (He, N_2, Ne, Hydrocarbons, Rn) and on the role of H_2-consuming microbial communities at the subsurface within the emitting structure (Myagkiy et al., 2020) [63] will be extremely valuable.

Author Contributions: All authors contributed to the writing of the paper. All authors have read and agreed to the published version of the manuscript.

Funding: The work reported here was not supported by any grant by any agency.

Acknowledgments: Grateful thanks to Guest Editor Lawrence Cathles and two anonymous reviewers for their constructive reviews. The first author would like to thank Sophie-Adélaïde Magnier for helpful discussions. Laurent Truche gratefully acknowledges the support from the Institut Universitaire de France.

Conflicts of Interest: The authors declare no conflict of interest.

References

1. Truche, L.; McCollom, T.M.; Martinez, I. Hydrogen and Abiotic Hydrocarbons: Molecules that Change the World. *Elem. Int. Mag. Miner. Geochem. Pet.* **2020**, *16*, 13–18. [CrossRef]
2. Smith, N.J.P. It's time for explorationists to take hydrogen more seriously. *First Break* **2002**, *20*, 246–253.
3. Smith, N.J.P.; Shepherd, T.J.; Styles, M.T.; Williams, G.M. Hydrogen exploration: A review of global hydrogen accumulations and implications for prospective areas in NW Europe. In *Petrology Geology: North-West Europe and Global Perspectives—Proceedings of the 6th Petroleum Geology Conference*; Doré, A.G., Vining, B.A., Eds.; Petroleum Geology Conference Series; Geological Society: London, UK, 2005; Volume 6, pp. 349–358.
4. Truche, L.; Bazarkina, E.F. Natural hydrogen the fuel of the 21st century. In *E3S Web of Conferences*; EDP Sciences: Les Ulis, France, 2019; Volume 98, p. 03006.
5. Gaucher, E.C. New Perspectives in the Industrial Exploration for Native Hydrogen. *Elem. Int. Mag. Miner. Geochem. Pet.* **2020**, *16*, 8–9. [CrossRef]
6. Zgonnik, V. The occurrence and geoscience of natural hydrogen: A comprehensive review. *Earth Sci. Rev.* **2020**, *203*, 103140. [CrossRef]
7. Neal, C.; Stanger, G. Hydrogen generation from mantle source rocks in Oman. *Earth Planet. Sci. Lett.* **1983**, *66*, 315–320. [CrossRef]
8. Coveney, R.M., Jr.; Goebel, E.D.; Zeller, E.J.; Angino, E.E. Serpentinization and the origin of hydrogen gas in Kansas. *AAPG Bull.* **1987**, *71*, 39–48.
9. Abrajano, T.A.; Sturchio, N.C.; Kennedy, B.M.; Lyon, G.L.; Muehlenbachs, K.; Bohlke, J.K. Geochemistry of reduced gas related to serpentinization of the Zambales ophiolite, Philippines. *Appl. Geochem.* **1990**, *5*, 625–630. [CrossRef]
10. Charlou, J.L.; Fouquet, Y.; Donval, J.P.; Auzende, J.M.; Jean-Baptiste, P.; Stievenard, M. Mineral and gas chemistry of hydrothermal fluids on an ultrafast spreading ridge: East Pacific Rise, 17° to 19°S (Naudur cruise, 1993) phase separation processes controlled by volcanic and tectonic activity. *J. Geophys. Res.* **1996**, *101*, 899–919. [CrossRef]
11. Seewald, J.S.; Cruse, A.; Saccocia, P. Aqueous volatiles in hydrothermal fluids from the Main Endeavour Field, northern Juan de Fuca Ridge: Temporal variability following earthquake activity. *Earth Planet. Sci. Lett.* **2003**, *216*, 575–590. [CrossRef]
12. Larin, N.; Zgonnik, V.; Rodina, S.; Deville, E.; Prinzhofer, A.; Larin, V.N. Natural molecular hydrogen seepage associated with surficial, rounded depressions on the European craton in Russia. *Nat. Resour. Res.* **2015**, *24*, 369–383. [CrossRef]
13. Zgonnik, V.; Beaumont, V.; Deville, E.; Larin, N.; Pillot, D.; Farrell, K.M. Evidence for natural molecular hydrogen seepage associated with Carolina bays (surficial, ovoid depressions on the Atlantic Coastal Plain, Province of the USA). *Prog. Earth Planet. Sci.* **2015**, *2*, 31. [CrossRef]
14. Prinzhofer, A.; Cissé, C.S.T.; Diallo, A.B. Discovery of a large accumulation of natural hydrogen in Bourakebougou (Mali). *Int. J. Hydrogen Energy* **2018**, *43*, 19315–19326. [CrossRef]
15. Prinzhofer, A.; Moretti, I.; Francolin, J.; Pacheco, C.; d'Agostino, A.; Werly, J.; Rupin, F. Natural hydrogen continuous emission from sedimentary basins: The example of a Brazilian H_2-emitting structure. *Int. J. Hydrogen Energy* **2019**, *44*, 5676–5685. [CrossRef]

16. Cathles, L.; Prinzhofer, A. What Pulsating H2 Emissions Suggest about the H2 Resource in the São Francisco Basin of Brazil. *Geosciences* **2020**, *10*, 149. [CrossRef]
17. Flude, S.; Warr, O.; Magalhães, N.; Bordmann, V.; Fleury, J.M.; Reis, H.L.S.; Trindade, R.I.; Hillegonds, D.; Sherwood Lollar, B.; Ballentine, C.J. Deep crustal source for hydrogen and helium gases in the São Francisco Basin, Minas Gerais, Brazil. *AGUFM* **2019**, *2019*, EP51D-2111.
18. Heilbron, M.; Cordani, U.G.; Alkmim, F.F. The São Francisco craton and its margins. In *São Francisco Craton 2017, Eastern Brazil*; Springer: Cham, Switzerland, 2017; pp. 3–13.
19. Anhaeusser, C.R. Archaean greenstone belts and associated granitic rocks—A review. *J. Afr. Earth Sci.* **2014**, *100*, 684–732. [CrossRef]
20. Teixeira, W.; Oliveira, E.P.; Marques, L.S. Nature and evolution of the Archean crust of the São Francisco Craton. In *São Francisco Craton 2017, Eastern Brazil*; Springer: Cham, Switzerland, 2017; pp. 29–56.
21. Delpomdor, F.R.; Ilambwetsi, A.M.; Caxito, F.A.; Pedrosa-Soares, A.C. New interpretation of the basal Bambuí Group, Sete Lagoas High (Minas Gerais, SE Brazil) by sedimentological studies and regional implications for the aftermath of the Marinoan glaciation: Correlations across Brazil and Central Africa. *Geol. Belg.* **2020**, *23*, 1. [CrossRef]
22. Curto, J.B.; Pires, A.C.; Silva, A.M.; Crósta, Á.P. The role of airborne geophysics for detecting hydrocarbon microseepages and related structural features: The case of Remanso do Fogo, Brazil. *Geophysics* **2012**, *77*, B35–B41. [CrossRef]
23. Solon, F.F.; Fontes, S.L.; Meju, M.A. Magnetotelluric imaging integrated with seismic, gravity, magnetic and well-log data for basement and carbonate reservoir mapping in the São Francisco Basin, Brazil. *Pet. Geosci.* **2015**, *21*, 285–299. [CrossRef]
24. Romeiro-Silva, P.C.; Zalán, P.V. Contribuição da sísmica de reflexão na determinação do limite oeste do Cráton do São Francisco. In Proceeding of the III Simpósio Sobre o Cráton do São Francisco, Salvador, Brazil, 14–18 August 2005; pp. 44–47.
25. Reis, H.L.; Alkmim, F.F. Anatomy of a basin-controlled foreland fold-thrust belt curve: The Três Marias salient, São Francisco basin, Brazil. *Mar. Pet. Geol.* **2015**, *66*, 711–731. [CrossRef]
26. Guélard, J.; Beaumont, V.; Rouchon, V.; Guyot, F.; Pillot, D.; Jézéquel, D.; Ader, M.; Newell, K.D.; Deville, E. Natural H2 in Kansas: Deep or shallow origin? *Geochem. Geophys. Geosyst.* **2017**, *18*, 1841–1865. [CrossRef]
27. Lin, L.H.; Hall, J.; Lippmann-Pipke, J.; Ward, J.A.; Sherwood Lollar, B.; DeFlaun, M.; Rothmel, R.; Moser, D.; Gihring, T.M.; Mislowack, B.; et al. Radiolytic H2 in continental crust: Nuclear power for deep subsurface microbial communities. *Geochem. Geophys. Geosyst.* **2005**, *6*, 1–13. [CrossRef]
28. Goebel, E.D.; Coveney, R.M.J.; Angino, E.E.; Zeller, E.J.; Dreschhoff, G.A.M. Geology, composition, isotopes of naturally occurring H2/N2 rich gas from wells near Junction City, Kansas. *Oil Gas J.* **1984**, *82*, 215–222.
29. Lollar, B.S.; Onstott, T.C.; Lacrampe-Couloume, G.; Ballentine, C.J. The contribution of the Precambrian continental lithosphere to global H 2 production. *Nature* **2014**, *516*, 379–382. [CrossRef] [PubMed]
30. Parnell, J.; Blamey, N. Global hydrogen reservoirs in basement and basins. *Geochem. Trans.* **2017**, *18*, 2. [CrossRef]
31. Reis, H.L.S.; Barbosa, M.S.C.; Alkmim, F.F.D.; Soares, A.C.P. Magnetometric and gamma spectrometric expression of southwestern São Francisco Basin, Serra Selada quadrangle (1:100.000), Minas Gerais state. *Rev. Bras. Geofísica* **2012**, *30*. [CrossRef]
32. Sighinolfi, G.P.; Figueredo, M.C.H.; Fyfe, W.S.; Kronberg, B.I.; Oliveira, M.T. Geochemistry and petrology of the Jequie granulitic complex (Brazil): An Archean basement complex. *Contrib. Mineral. Petrol.* **1982**, *78*, 263–271. [CrossRef]
33. Donatti-Filho, J.P.; Tappe, S.; Oliveira, E.P.; Heaman, L.M. Age and origin of the Neoproterozoic Brauna kimberlites: Melt generation within the metasomatized base of the São Francisco craton, Brazil. *Chem. Geol.* **2013**, *353*, 19–35. [CrossRef]
34. Lin, L.H.; Slater, G.F.; Lollar, B.S.; Lacrampe-Couloume, G.; Onstott, T.C. The yield and isotopic composition of radiolytic H2, a potential energy source for the deep subsurface biosphere. *Geochim. Cosmochim. Acta* **2005**, *69*, 893–903. [CrossRef]
35. Schlindwein, V.; Schmid, F. Mid-ocean-ridge seismicity reveals extreme types of ocean lithosphere. *Nature* **2016**, *535*, 276–279. [CrossRef]
36. Horning, G.; Sohn, R.A.; Canales, J.P.; Dunn, R.A. Local seismicity of the rainbow massif on the Mid-Atlantic Ridge. *J. Geophys. Res. Solid Earth* **2018**, *123*, 1615–1630. [CrossRef]

37. Foustoukos, D.I.; Savov, I.P.; Janecky, D.R. Chemical and isotopic constraints on water/rock interactions at the Lost City hydrothermal field, 30 N Mid-Atlantic Ridge. *Geochim. Cosmochim. Acta* **2008**, *72*, 5457–5474. [CrossRef]
38. Proskurowski, G.; Lilley, M.D.; Seewald, J.S.; Früh-Green, G.L.; Olson, E.J.; Lupton, J.E.; Sylva, S.P.; Kelley, D.S. Abiogenic hydrocarbon production at Lost City hydrothermal field. *Science* **2008**, *319*, 604–607. [CrossRef]
39. Coelho, J.C.C.; Martins-Neto, M.A.; Marinho, M.S. Estilos estruturais e evolução tectônica da porção mineira da bacia proterozóica do São Francisco. *Rev. Bras. Geociências* **2008**, *38* (Suppl. S2), 149–165. [CrossRef]
40. Alkmim, F.F.; Martins-Neto, M.A. Proterozoic first-order sedimentary sequences of the São Francisco craton, eastern Brazil. *Mar. Pet. Geol.* **2012**, *33*, 127–139. [CrossRef]
41. Reis, H.L.; Suss, J.F.; Fonseca, R.C.; Alkmim, F.F. Ediacaran forebulge grabens of the southern São Francisco basin, SE Brazil: Craton interior dynamics during West Gondwana assembly. *Precambrian Res.* **2017**, *302*, 150–170. [CrossRef]
42. Reis, H.L.; Alkmim, F.F.; Fonseca, R.C.; Nascimento, T.C.; Suss, J.F.; Prevatti, L.D. The São Francisco Basin. In *São Francisco Craton, Eastern Brazil*; Springer: Cham, Switzerland, 2017; pp. 117–143.
43. Chemale, F., Jr.; Dussin, I.A.; Alkmim, F.F.; Martins, M.S.; Queiroga, G.; Armstrong, R.; Santos, M.N. Unravelling a Proterozoic basin history through detrital zircon geochronology: The case of the Espinhaço Supergroup, Minas Gerais, Brazil. *Gondwana Res.* **2012**, *22*, 200–206. [CrossRef]
44. Oliveira, R.G.; Andrade, J.B.F. Interpretação Geofísica dos Principais Domínios Tectônicos Brasileiros. In *Metalogênese da Províncias Tectônicas Brasileiras*, 1st ed.; Silva, M.G., Rocha Neto, M.B., Jost, H., Kuyumjian, R.M., Eds.; CPRM—Serviço Geológico do Brasil: Rio de Janeiro, Brazil, 2014; Volume 1, pp. 21–38.
45. Pereira, R.S.; Fuck, R.A. Archean nucleii and the distribution of kimberlite and related rocks in the São Francisco craton, Brazil. *Rev. Bras. Geociências* **2016**, *35* (Suppl. S4), 93–104. [CrossRef]
46. Correa, R.T. *Mapa da Anomalia Magnética do Brasil (Terceira Edição)*; Escala 1:5.000.000; SGB-CPRM—Serviço Geológico do Brasil: Brasília, Brazil, 2019.
47. Pinto, L.G.R.; Ussami, N.; Sá, N.C.D. Aquisição e interpretação de anomalias gravimétricas do Quadrilátero Ferrífero, SE do Cráton São Francisco. *Rev. Bras. Geofísica* **2007**, *25*, 21–30. [CrossRef]
48. Alexandrino, C.H.; Hamza, V.M. Estimates of heat flow and heat production and a thermal model of the São Francisco craton. *Int. J. Earth Sci.* **2008**, *97*, 289–306. [CrossRef]
49. Klein, F.; Bach, W.; McCollom, T.M. Compositional controls on hydrogen generation during serpentinization of ultramafic rocks. *Lithos* **2013**, *178*, 55–69. [CrossRef]
50. Mayhew, L.E.; Ellison, E.T.; McCollom, T.M.; Trainor, T.P.; Templeton, A.S. Hydrogen generation from low-temperature water–rock reactions. *Nat. Geosci.* **2013**, *6*, 478–484. [CrossRef]
51. Miller, H.M.; Mayhew, L.E.; Ellison, E.T.; Kelemen, P.; Kubo, M.; Templeton, A.S. Low temperature hydrogen production during experimental hydration of partially-serpentinized dunite. *Geochim. Cosmochim. Acta* **2017**, *209*, 161–183. [CrossRef]
52. Alexandrino, C.H.; Hamza, V.M. Improved assessment of Deep Crustal Thermal Field based on Joint Inversion of Heat Flow, Elevation and Geoid Anomaly data. *Geophys. Res. Abstr.* **2012**, *13*, EGU2011-10079.
53. Kennedy, B.M.; Kharaka, Y.K.; Evans, W.C.; Ellwood, A.; DePaolo, D.J.; Thordsen, J.; Ambats, G.; Mariner, R.H. Mantle fluids in the San Andreas fault system, California. *Science* **1997**, *278*, 1278–1281. [CrossRef]
54. Donzé, F.V.; Tsopela, A.; Guglielmi, Y.; Henry, P.; Gout, C. Fluid migration in faulted shale rocks: Channeling below active faulting threshold. *Eur. J. Environ. Civ. Eng.* **2020**, 1–15. [CrossRef]
55. Truche, L. Transformations Minéralogiques et Géochimiques Induites par la Présence D'hydrogène dans un site de Stockage de Déchets Radioactifs. Ph.D. Thesis, Université de Toulouse, Université Toulouse III-Paul Sabatier, Toulouse, France, 2009.
56. De Carvalho, O.A.; Guimarães, R.F.; Montgomery, D.R.; Gillespie, A.R.; Trancoso Gomes, R.A.; de Souza Martins, É.; Silva, N.C. Karst depression detection using ASTER, ALOS/PRISM and SRTM-derived digital elevation models in the Bambuí Group, Brazil. *Remote Sens.* **2014**, *6*, 330–351. [CrossRef]
57. Dos Santos, D.M.; Sanchez, E.A.; Santucci, R.M. Morphological and petrographic analysis of newly identified stromatolitic occurrences in the Lagoa do Jacaré Formation, Bambuí Group, State of Minas Gerais, Brazil. *Rev. Bras. Paleontol.* **2018**, *21*, 3. [CrossRef]
58. Galvão, P.; Halihan, T.; Hirata, R. The karst permeability scale effect of Sete Lagoas, MG, Brazil. *J. Hydrol.* **2016**, *532*, 149–162. [CrossRef]

59. Bazarkina, E.F.; Chou, I.M.; Goncharov, A.F.; Akinfiev, N.N. The Behavior of H2 in Aqueous Fluids under High Temperature and Pressure. *Elem. Int. Mag. Mineral. Geochem. Petrol.* **2020**, *16*, 33–38. [CrossRef]
60. Charlou, J.L.; Donval, J.P.; Konn, C.; OndréAs, H.; Fouquet, Y.; Jean-Baptiste, P.; Fourré, E. High production and fluxes of H_2 and CH_4 and evidence of abiotic hydrocarbon synthesis by serpentinization in ultramafic-hosted hydrothermal systems on the Mid-Atlantic Ridge. *GMS* **2010**, *188*, 265–296.
61. Keir, R.S. A note on the fluxes of abiogenic methane and hydrogen from mid-ocean ridges. *Geophys. Res. Lett.* **2010**, *37*. [CrossRef]
62. Cannat, M.; Fontaine, F.; Escartin, J. Serpentinization and associated hydrogen and methane fluxes at slow spreading ridges. In *Diversity of Hydrothermal Systems on Slow Spreading Ocean Ridges*; Rona, P.A., Devey, C.W., Dyment, J., Murton, B.J., Eds.; AGU Geophysical Monograph Series; John Wiley and Sons: Hoboken, NJ, USA, 2010; Volume 188.
63. Myagkiy, A.; Brunet, F.; Popov, C.; Krüger, R.; Guimarães, H.; Sousa, R.S.; Charlet, L.; Moretti, I. H2 dynamics in the soil of a H2-emitting zone (São Francisco Basin, Brazil): Microbial uptake quantification and reactive transport modelling. *Appl. Geochem.* **2020**, *112*, 104474. [CrossRef]